THREE-DIMENSIONAL VIEWS OF TITAN'S DIVERSE SURFACE FEATURES FROM CASSINI RADAR STEREOGRAMMETRY. R.L. Kirk[1], E. Howington-Kraus[1], B.L. Redding[1], T.L. Becker[1], E.M. Lee[1], B.W. Stiles[2], S. Hensley[2], A.G. Hayes[3], R.M.C. Lopes[2], R.D. Lorenz[4], K.L. Mitchell[2], J. Radebaugh[5], F. Paganelli[6], L.A. Soderblom[1], E.R. Stofan[6], C.A. Wood[7], S.D. Wall[2], and the Cassini RADAR Team, [1]U.S. Geological Survey, Astrogeology Program, Flagstaff, AZ 86001 (rkirk@usgs.gov), [2]Jet Propulsion Laboratory, Pasadena, CA 91109, [3]Caltech, Pasadena, CA, 91125, [4]Johns Hopkins University Applied Physics Lab, Laurel, MD 20723, [5]Brigham Young University, Provo, UT 84602, [6]Proxemy Research, Gaithersburg, MD 20882, [7]Wheeling Jesuit University, Wheeling, WV 26003.

Introduction: As of the end of the Cassini Prime Mission, the RADAR instrument [1] has imaged ~27% of Titan's surface with "main swath" synthetic aperture radar (SAR) coverage at resolutions of 0.3–1.5 km and an additional 7% with high-altitude SAR images having ~2 km resolution [2]. This image set includes overlapping coverage of 1–2% of Titan that can be analyzed by radar stereogrammetric techniques to yield topographic information with horizontal resolutions of few tens of km and vertical precision on the order of 100 m or better. We have previously described the topography of a handful of areas on Titan, based on qualitative [3] and preliminary quantitative [4] examination of some of the first RADAR stereo pairs. We are currently collecting digital topographic models (DTMs) of all stereo overlap areas (currently >20, with more accumulating during the Cassini Extended Mission). Our mapping effort has been made possible, in part, by completion of the software tools needed for both interactive and automated stereoanalysis of the RADAR data at the USGS [5]. Another key factor has been the reprocessing of the entire RADAR dataset, based on an improved model of Titan's rotation [6], which reduced the positional mismatches between overlapping images from tens of km to uniformly less than 1 km. Stereoanalysis of the reprocessed images provides at least a partial check on absolute as well as relative elevations obtained by other observations such as altimetry [7] and SAR topo [8]. In this abstract, we summarize the results of stereo topographic mapping of several newly mapped areas of Titan.

Methodology: To perform stereo analysis of Cassini SAR data, the USGS uses the software package SOCET SET® available from BAE Systems [9]. The in-house cartographic software package ISIS [10] is used to prepare the images and supporting metadata in formats that the commercial software can understand. SOCET SET provides many useful capabilities, including bundle adjustment (least-squares adjustment of the spacecraft trajectories to improve the alignment of the images and bring the topographic results into agreement with *a priori* data such as SAR topography elevations); creation of DTMs with powerful and highly adjustable image matching algorithms; and manual quality control, editing, or even *ab initio* creation of DTMs. Interactive processing makes use of a stereo monitor to display the images simultaneously with the DTM. Given the challenging properties of the RADAR images for stereo matching (modest image size, speckle noise, and differences in illumination between the images), the ability to make interactive measurements is essential. Most of the DTMs presented here were refined by automatic matching after manual "seeding" with a sparse set of height measurements, but in some cases automated matching was not successful and our DTMs were obtained wholly by manual measurement.

The functions just described require a "sensor model," i.e., software that calculates the image pixel that corresponds to a given ground location in latitude, longitude, and elevation, or the reverse. We used the SOCET Developer's Toolkit (Devkit) to implement such a sensor model for the Cassini RADAR. This model emulates the physical process of SAR image formation in a rigorous way, and distinguishes the nominal spacecraft trajectory used in making the SAR images from the improved trajectory that is estimated in the bundle adjustment process [4, 5].

Results: The SAR image pairs from which we have produced DTMs are summarized in Table 1, which includes the estimated vertical precision (EP) based on the incidence angles i_1 and i_2 at a representative point, the angle α at which the swaths cross, and a nominal value of 351 m for the accuracy with which features can be matched between images. This matching accuracy is conservative; it is roughly the intrinsic resolution of the best images, but the pixel scale is a factor of 2 smaller and subpixel matching accuracy is routinely obtained in stereo mapping. Replicate manual measurements of selected features in one pair (T8-T25) were found to vary by ~25 m RMS in height, or about 1/4 of the tabulated EP. This suggests that matching is repeatable, if not necessarily accurate, to a subpixel level. In any case, the table indicates the vertical precision of different DTMs in at least a relative sense.

T25-T28 We presented an initial DTM for Mayda Insula, a 90x150 km island in the largest of Titan's north polar seas, Kraken Mare, a year ago [4]; the full area of overlap of these images has since been mapped [5]. The most basic discovery is that the darkest areas occupy the topographic lows, consistent with their interpretation as lakes and seas of liquid hydrocarbons [11]. The highest recorded elevations are about 1200 m above the shorelines, placing at least loose constraints on the probable depth of the seas, and thus on the liquid hydrocarbon inventory [12]. Stereo elevations computed without bundle adjustment agreed well with SAR topo in most areas, with a mean difference of 70 m and standard deviation of 140 m; the latter indicates that the matching error is indeed smaller than the image resolution. A larger discrepancy was found along the coast of Mayda Insula, where the SAR topo method is likely to have been biased by the strong image contrast.

T8-T21 These images cross at a high angle in the equatorial "sand sea" Belet and include both dark longitudinal dunes and brighter, dune-free areas [13]. The relief visible in stereo is subtle, but consistent topographic results were obtained by manual measurement, automated image matching, and a combination of both. Dune-free areas were found to be consistently higher than the dunes, with typical relief at the boundary of ~200 m; pockets of dark sediment were found to occupy local depressions in the highlands. The similar appearance of the dunes in images illuminated from different directions suggests that we are mainly seeing the intrinsic contrast between dunes and interdunes here rather than shading of the dune slopes [14], so that the elevations measured by stereo matching should be representative of the bases of the dunes. Thus, it seems likely that ~200 m of relief is sufficient to divert the dunes. Individual dunes are not resolved in the DTM, but it is possible to make interactive measurements of the largest ones. The heights, ~100–150 m, are consistent with past estimates from radarclinometry applied to dunes elsewhere that show clear topographic shading [13].

T8-T41 This pair resembles T8-T21 closely; it is of interest because it contains the Huygens landing site. Here, too, bright areas are found to be elevated by a few hundred meters above the dune fields. Though not covered by dunes, the landing site is in a valley 180–300 m lower than the radar-bright "islands" to its north and south. This result is consistent with the local relief of 250 m measured for the highland north of the landing site based on Huygens DISR stereo images [15]. The RADAR DTM shows a regional slope of about 0.2° to the northeast, and a steeper slope of 0.4° in the same direction at the landing site. The regional slope is not present in SAR topo data, the only case so far of

such a gross disagreement. Even if the DTM were to be adjusted to remove this overall slope, however, the local slope to the northeast near the landing site is consistent with the flow features identified in the DISR images [15].

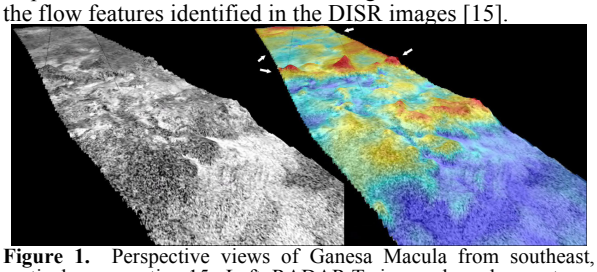

Figure 1. Perspective views of Ganesa Macula from southeast, vertical exaggeration 15. Left, RADAR Ta image draped over stereo DTM. Right, image colored with elevation. Range from blue (low) to red (high) is 1000 m. Arrows indicate low western and elevated eastern margins of Ganesa.

Ta-T23 The overlap between these images extends from 14°–98° W longitude, but our initial DTM covers a smaller region around Ganesa Macula. This 180-km quasi-circular feature identified in the first RADAR image of Titan [16] somewhat resembles steep-sided domes on Venus and has been hypothesized to be a cryovolcanic construct [17]. SAR topo profiles [8] do not show the feature to be consistently elevated, though there is a strong drop-off at its eastern edge. The stereo DTM (Figure 1) is consistent with these profiles but provides additional information. Ganesa as a whole is tilted, low along its western edge and generally (but not uniformly) elevated in the east. The western low and the scarp bounding a ~600 m deep trough to the east of Ganesa both continue to the southern edge of stereo coverage rather than following the curved southern boundary of the feature itself. A second, even deeper trough lies to the east. Both the mountains separating these two troughs and Ganesa itself appear to be dissected, with bright channels and flow features [16] occupying local lows between highlands that are darker. Thus, although Ganesa may have originated as a cryovolcanic feature or an impact crater (either of which would account for its distinct circular outline), little or no topographic expression of a dome or shield is seen. The feature appears to have been extensively modified by both tectonic processes (as indicated by the alternating highs and lows with north-south trending boundaries) and fluvial erosion (the bright channels and flow deposits) [21].

T41-T43 This pair covers part of Hotei Arcus, a 650-km semicircular feature that is unusually bright at 5 µm in the infrared [18] and may be time-variable [19]. RADAR images of Hotei show rugged terrain along the arc itself, lobate bright and dark features that have been interpreted as cryovolcanic flows to the immediate west, and radar-bright channels that may be fluvial in between [20]. The stereo DTM (Figure 2) confirms that the rugged areas are elevated and clarifies the relations between the bright and dark lobate features. Individual flows range from 100–200 m in thickness, with dark margins and bright, somewhat mottled top surfaces, on a more uniformly radar-bright substrate. These thick flows imply a cryolava of significant viscosity, a conclusion that can be quantified by modeling that takes into account the driving slopes (also derivable from the DTM). The bright channels, in contrast, are incised into the mountains and display little elevation change, consistent with a lower viscosity fluid such as pluvial/fluvial liquid methane.

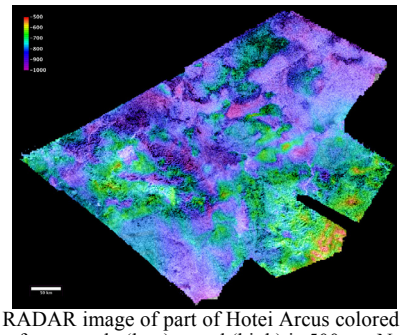

Figure 2. RADAR image of part of Hotei Arcus colored with elevation. Range from purple (low) to red (high) is 500 m. North at top.

T13-T43 This pair covers part of the "middle rugged terrain" of north central Xanadu [22]. The DTM does not resolve the many small (<10 km across) mountains across the region, but clearly shows the largest peaks and chains to be elevated by hundreds of meters. The model also indicates a regional slope of ~0.1° to the southwest, consistent with the apparent flow direction of numerous fluvial channels in western Xanadu [22]. The stereo results need to be considered in conjunction with radarclinometry, which indicates local relief of 1000 m or more for the individual mountains but does not address variations over distances longer than about 10 km [22, 23].

Future Work: The results reported here (without bundle adjustment) have reasonable agreement in absolute elevation with SAR topo data: 100–300 m mean offset, ~100 m RMS variation. In the near future, we intend to adjust the images to improve and better quantify the level of agreement. The main task before us, however, is to produce (and interpret!) additional DTMs. We look forward to presenting quantitative results and three-dimensional "flyover" visualizations for additional areas in our talk, some of the most interesting of which are a high resolution stereo transect from the polar seas to 20°S (T25-T28-T29), additional cryovolcanic flow features (remainder of Ta-T23), numerous small lakes and the rim of a possible 300-km impact crater (T16-T19), western Xanadu (T13-T44), a mountainous area near 35° S (T7-T39), and Tui Regio, another 5-µm-bright area of possible cryovolcanic flows (T43-T48).

References: [1] Elachi, C. et al. (2004) *Space Sci. Rev., 115*, 71. [2] West, R.D., et al. (2008) *Eos Trans. AGU, 89*(53), P21a-1347. [3] Kirk, R.L. et al. (2007) *LPS XXXVIII,* 1427. [4] Kirk, R.L. et al. (2008) *LPS XXXIX,* 2320. [5] Kirk, R.L., et al. (2008) *IAPRSSIS, XXXVII*(4), 973. [6] Stiles, B.W. et al. (2008) *Astron. J., 135*, 1669. [7] Zebker, H.A. et al. (2009) *Icarus*, submitted. [8] Stiles, B.W. et al. (2009) *Icarus*, submitted. [9] Miller, S.B., and A.S. Walker (1993) *ACSM/ASPRS Ann. Conv., 3*, 256; (1995) *Z. Phot. Fern. 63*, 4. [10] Eliason, E. (1997) *LPS XXVIII*, 331; Gaddis, L.R. et al. (1997) *LPS XXVIII*, 387; Torson, J., and K. Becker, (1997) *LPS XXVIII*, 1443. [11] Stofan, E. et al. (2007) *Nature, 445,* 61. [12] Lorenz, R.D., et al. (2008) *GRL, 15*, L02206. [13] Lorenz, R.D., et al. (2006) *Science*, *312*, 724. [14] Paganelli, F. et al. (2008) *Eos Trans. AGU, 89*(53), P21A-1311. [15] Soderblom, L.A. et al. (2007) *PSS, 55*, 2015. [16] Elachi, C. et al. (2005) *Science, 308*, 970. [17] Lopes, R.M.C. et al. (2007) *Icarus, 187*, 395. [18] Barnes et al. (2005) *Science 310*, 92. [19] Nelson, R.M. et al. (2009) *GRL*, in press. [20] Wall, S.D. et al. (2009) GRL, in press. [21] Mitchell, K.L. et al. (2009) *LPS XD*, this conference. [22] Radebaugh, J. et al. (2009) *Icarus*, submitted. [23] Radebaugh, J. et al. (2007) *Icarus*, *192*, 77.

Table 1—Cassini RADAR Stereo Pairs Mapped

Image 1 (Titan Flyby)	Image 2	Inc angle i_1	Inc angle i_2	Crossing angle α	Precision EP (m)	West Longitude Range	Latitude Range
T25	T28	11°	19°	~0°	157	-95°–11°	59°–77°
T8	T21	19°	15°	65°	97	285°–295°	-13°– -6°
T8	T41	18°	11°	40°	103	186°–202°	-17°– -6°
Ta	T23	32°	23°	~180°	90	63°–96°	47°–53°
T41	T43	21°	22°	125°	78	75°–91°	-35°– -24°
T13	T43	25°	20°	30°	252	99°–120°	-13°– -8°